

## Self-powered environmental sensor system driven by nanogenerators†

 Minbaek Lee,‡<sup>a</sup> Joonho Bae,‡<sup>a</sup> Joohyung Lee,<sup>b</sup> Churl-Seung Lee,<sup>c</sup> Seunghun Hong<sup>b</sup> and Zhong Lin Wang\*<sup>a</sup>

Received 27th April 2011, Accepted 26th May 2011

DOI: 10.1039/c1ee01558c

**We demonstrate a fully stand-alone, self-powered environmental sensor driven by nanogenerators with harvesting vibration energy. Such a system is made of a ZnO nanowire-based nanogenerator, a rectification circuit, a capacitor for charge storage, a signal transmission LED light and a carbon nanotube-based Hg<sup>2+</sup> ion sensor. The circuit lights up the LED indicator when it detects mercury ions in water solution. It is the first demonstration of a nanomaterial-based, self-powered sensor system for detecting a toxic pollutant.**

A self-powered sensor for toxic materials could be the most desirable and promising prototype of future monitoring systems for environmental protection/detection. Wiring a power-source to sensors that are placed in every corner of our surroundings not only causes a vast amount of labour, resources and budget, but also causes potential contamination to be produced by the batteries. Although solar energy is most attractive, it depends on the weather, season and has

day and night difference. However, regardless of day and night, mechanical energy is one of the most abundant/sustainable sources practically to be utilized through piezoelectric materials.<sup>1–8</sup> ZnO nanowires (NWs) not only exhibit piezoelectricity,<sup>9–11</sup> but also are environmentally friendly and biologically compatible,<sup>12–15</sup> which make it a strong candidate for energy-harvesting as environmental sensors. In previous work, piezoelectric nanogenerators (NGs) based on vertically or horizontally aligned ZnO NW arrays have been demonstrated for driving an ultraviolet (UV) sensor<sup>5</sup> and a laser emitting diode (LED).<sup>6</sup>

Compared to an UV sensor in previous work that needed auxiliary supports from signal amplifiers because of small signal output, we report an enhanced environmental sensor capable of operating solely by itself without a battery to detect toxicity without the support of additional equipment. In the fabrication of high performance NGs, flexible Kapton was utilized as a substrate to enlarge the number of effective contacts between the ends of the piezoelectric ZnO NWs and the Au electrodes. Once the NWs are uniaxially compressed, a piezoelectric potential drop is created along their lengths, which drives the flow of electrons in the external load.<sup>5</sup> A dynamic and cycled compressing and releasing of strain over the NWs results in a synchronized back and forth flow of electrons. The produced alternating electrical output is rectified and stored in a super-capacitor/capacitor for the operation of the sensor. The environmental sensor was composed of single-walled carbon nanotube (SWNT) networks. We intentionally chose SWNT field effect transistors (FETs) with *enhancement-mode*<sup>16</sup> to effectively use the stored electricity for sensing. When mercury ions in water approached the SWNT FET, it turns on the FET,<sup>17,18</sup> which allows current flow in the circuit. Finally, the attached LED will be lit up with the different

<sup>a</sup>School of Material Science and Engineering, Georgia Institute of Technology, Atlanta, GA, 30332, USA. E-mail: zhong.wang@mse.gatech.edu; Fax: +1 404 384 3852; Tel: +1 404 894 8008

<sup>b</sup>Department of Physics and Astronomy, Seoul National University, Seoul, 151–747, Korea

<sup>c</sup>Nano technology based Information and Energy Storage Research Center, Korea Electronics Technology Institute, Seongnam-si, Gyeonggi-do, 463–816, Korea

† Electronic supplementary information (ESI) available: Materials for supporting the conclusions and discussions presented in the main text, including the experimental methods, explanation of high performance nanogenerator and switching polarity test. See DOI: 10.1039/c1ee01558c

‡ These authors contributed equally to this work.

### Broader context

A self-powered sensor system for toxic pollutants could be the most attractive platform of future monitoring devices for environmental protection/detection. Aside from solar energy which depends on the weather and circumstance, mechanical energy is one of the most easily accessible sources, which can be harvested *via* piezoelectric materials. In this regard, the ZnO nanowire is a very suitable candidate because it is known to be piezoelectric and relatively non-toxic to environments as well. By employing a ZnO nanowire as an energy harvesting part, the first demonstration of a self-powered sensor system for detecting a toxic pollutant is presented here. Such a system is made of a ZnO nanowire-based nanogenerator, a rectification circuit, a capacitor for charge storage, a signal transmission LED light and a carbon nanotube-based sensor. Depending on the concentration of the pollutant, the circuit is designed to light up the LED indicator with different intensities using harvested energy. The LED indicator may be replaced by an RF unit in the future so that the signal can be detected wirelessly over a longer distance. Furthermore, it may inspire the development of a future self-powered sensor for unreachable or access-denied extreme environments.

intensities depending on the concentration of toxic materials. Significantly, the entire detection of environmental pollutant and indication of the result have been successfully demonstrated utilizing only energy stored by NGs. This demonstration can be a practical and versatile prototype for self-powered, stand-alone environmental sensors in the future.

In the fabrication of high performance NGs, two simple but effective principles were applied here. One is stacking of multiple NGs along the *c*-axis of NWs,<sup>5</sup> and the other is employment of flexible substrates to enhance the number of effective NWs in the generator. According to previous reports,<sup>3,5,6</sup> NWs with wurtzite crystal structure are known to grow uniaxially parallel to the *c*-axis. This growth property of the NWs allows us to easily integrate multiple NGs based on ZnO NWs along the *c*-axis or parallel to the *c*-axis.<sup>5,6</sup> Crystallographic alignment of NWs in NGs is very important because it determines the displacement of ionic distribution in the crystal which eventually results in averaged piezoelectric potential on the macroscopic scale. Besides a stacking method of multiple NGs, the density of 'effective NWs' in NGs is also a significant parameter to affect their output power. In a NG, we can define 'effective NWs' as fully contacting NWs in between two electrodes (see ESI, Fig. S1†). When an external stress is applied, only contacted NWs can be effectively under compression/pressure, so that they contribute a potential difference between the two electrodes. To increase the number of contacting NWs in the generator, we employed flexible Kapton layers as substrates for both the ZnO NW array and Au electrode. Flexible substrates can follow the height profiles of the NW forest and make effective contacts between the ends of NWs and electrodes (see ESI, Fig. S1b†). Fig. 1 shows scanning electron microscope (SEM) images

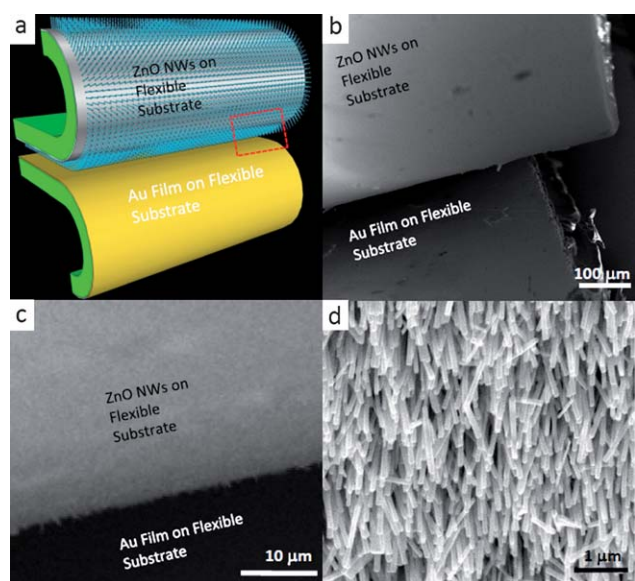


**Fig. 1** Schematic diagram and scanning electron microscope (SEM) images of the fabricated nanogenerator. (a) Schematic diagram depicting the structure of a fabricated nanogenerator on flexible substrates. Both the ZnO NW array and Au film were made on Kapton substrates with high flexibility. (b) Low magnification SEM image of a junction between the ZnO NW array and Au film of a fabricated nanogenerator. (c) Intermediate magnification SEM image of a junction between the ZnO NW array and Au film of a fabricated nanogenerator. (d) High magnification SEM image of a ZnO NW array. The ZnO NW forest shows only moderate alignment.

of a fabricated device and a schematic diagram depicting the ZnO NW array and Au film ( $\sim 50$  nm) on the flexible substrate. Because flexible Kapton layers ( $\sim 50.8$   $\mu\text{m}$ ) served as substrates for all parts in our fabrication, it can be freely bent or deformed as depicted schematically in Fig. 1a. Scanning electron microscopy (SEM) was exploited for the observation of the ZnO NW array on flexible substrates. Fig. 1b and d show SEM images of a bent-area at different magnifications. In Fig. 1d, ZnO NWs show a clear crystal shape that represents their single crystalline structure.

Fig. 2a and b show open-circuit voltage and closed-circuit current, respectively. A single NG with a surface area of  $\sim 0.8$   $\text{cm}^2$  reached an output voltage of  $\sim 350$  mV and a current of  $\sim 125$   $\text{nA cm}^{-2}$ . These values are much higher than those of a previous report.<sup>5</sup> The enhanced voltage and current outputs from our NGs can be attributed to the fact that our NGs on the flexible substrate are able to make a much improved number of contacts between NWs and electrode. When the hydrothermal growth method is employed,<sup>19</sup> it is a difficult task to grow a fully aligned/uniform ZnO NW array without any additional process such as e-beam lithography, photolithography or laser patterning. Non-uniformity of the NW array is a problematic phenomenon for the application to NGs because it results in few active contacts between metal electrode and NWs on the solid substrate (see Fig. S1a in the ESI†). This limitation can be resolved by replacing solid substrates with flexible ones, thus those can follow the morphology of a relatively non-uniform NW array (see Fig. S1b in the ESI†). As a proof of concept, insets in Fig. 2a and

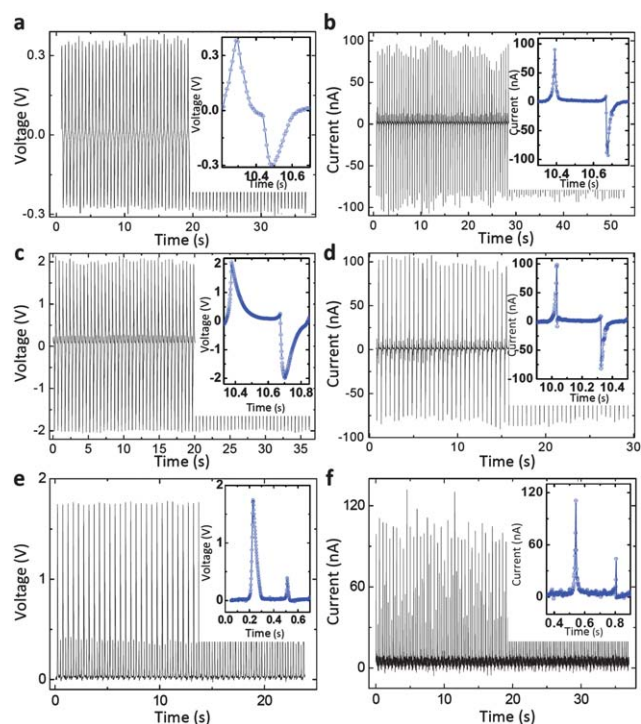


**Fig. 2** Electrical characteristics of fabricated nanogenerators as they are periodically strained and released. (a) Open-circuit voltage output of a fabricated nanogenerator. (b) Closed-circuit current output of a fabricated nanogenerator. (c) Open-circuit voltage output of ten-layer integrated nanogenerators. (d) Closed-circuit current output of ten-layer integrated nanogenerators. (e) Rectified open-circuit voltage output of ten-layer integrated nanogenerators. (f) Rectified closed-circuit current output of ten-layer integrated nanogenerators.

b clearly show enhanced power outputs from a NG on the flexible substrate. Serial stacking/connecting of NGs is an effective method for increasing the output voltage. Fig. 2c and d show output signals from a 10-layer integrated NG device. The open-circuit voltage and closed-circuit current reach up to  $\sim 2.1$  V and  $\sim 105$  nA (a peak output power density of  $\sim 0.3$  mW cm $^{-2}$ ), respectively. They are enough to use a rectifying circuit to store the NG output in any storage system. After integration of NGs and rectifying parts, we could observe almost the same amount of current output and a slightly reduced voltage output from NGs. Dissipation of voltage was caused by a rectifying circuit containing four diodes. The high performance of our NGs was due to the flexibility of substrates which enhanced the number of contacts between piezoelectric sources and metal electrodes.

Integration of NGs with an energy storage device such as a super-capacitor can be a prototype of a power cell for periodically acetyfied sensing devices that usually have a relatively long standby mode and a short active mode. During hibernation of the sensor, generated electricity from the NG is able to be stored in a super-capacitor. When the sensor needs to be operated, the stored energy in a super-capacitor/capacitor will supply the electric power for detection of environmental pollutants. To achieve this, we first fabricated a super-capacitor based on multi-walled CNT (MWNT) coated ITO electrodes<sup>20</sup> and PVA/H<sub>3</sub>PO<sub>4</sub> electrolyte.<sup>21</sup> The direct spray coating method was applied to make uniformly dispersed MWNT layers on ITO glass substrates (Fig. 3a).<sup>20</sup> MWNT coated ITO glass substrates served as working and counter electrodes for a super-capacitor. The PVA/H<sub>3</sub>PO<sub>4</sub> polymer like solution was used as electrolyte. The right upper inset in Fig. 3a shows a schematic diagram depicting the structure of a super-capacitor fabricated here. The electrochemical properties of the capacitors in the PVA/H<sub>3</sub>PO<sub>4</sub> electrolyte solution were investigated using a potentiostat/galvanostat (Princeton Applied Research VersaStat 3F). Fig. 3b exhibits cyclic voltammetry that

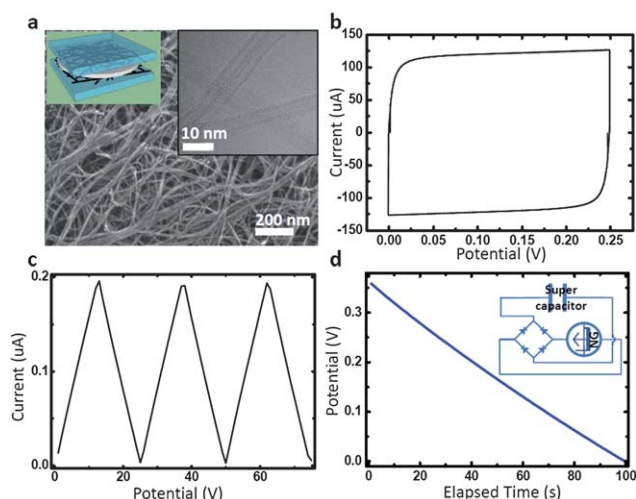


**Fig. 3** Characteristics of a multi-walled carbon nanotube based super-capacitor and storage test using a nanogenerator. (a) Schematic diagram and SEM/TEM images of a carbon nanotube network based super-capacitor. (b) Cyclic voltammetry of a fabricated super-capacitor. The scan range was between 0 and 250 mV with scan rates of 100 mV s $^{-1}$ . (c) Galvanostatic charge-discharge graph of the super-capacitor. (d) Discharging graph of a super-capacitor, which was charged by ten-layer integrated nanogenerators for  $\sim 1$  h.

shows our device has a good electrochemical stability and capacitance. The scan range was between 0 and 250 mV with scan rates of 100 mV s $^{-1}$ . The galvanostatic charge-discharge measurement was also conducted to characterize the electrochemical performance of the MWNT-based super-capacitor (Fig. 3c). To store the generated charge from NGs, a super-capacitor and 10-layer-integrated NGs were connected with a rectifying bridge (inset in Fig. 3d). The generated AC outputs from NGs were rectified into direct-current (DC) signals, which directly resulted in the charging process in a super-capacitor. After charging for  $\sim 1$  h by applying mechanical vibration to NGs with a frequency of 10 Hz and a displacement of  $\sim 1.2$  cm (Labworks Inc.), a discharge measurement was conducted to evaluate the stored energy. It was found that the accumulated amount of charge was  $\sim 3.6 \times 10^{-4}$  C, ensuring that we could apply it to an environmental sensing system. It implies that high output NGs might not be appropriate to power a continuously working sensor, but those can power an environmental sensor which detects pollutants periodically.

It is more desirable to have a sensor system that is not only wireless, mobile and extremely small, but also self-powered and sustainable. To achieve those requirements, we have fabricated a self-powered environmental sensor, which can detect Hg<sup>2+</sup> ions and indicate its concentration *via* the intensity of an LED. A single-walled CNT (SWNT) based FET and ZnO NW array served as Hg<sup>2+</sup> sensor and energy harvesting part, respectively. A SWNT network based sensor array was fabricated in a 4 inch wafer by using the chemical patterning method reported before.<sup>18,22,23</sup> Fig. 4a shows a photograph image of a fabricated sensor array on a 4 inch SiO<sub>2</sub> wafer. SWNT network based FETs can be in either *enhancement mode* or *depletion mode* since the network is composed of metallic and semiconducting SWNTs. In our sensor fabrication, the density of SWNT networks was intended to be relatively low (Fig. 4b) because networks with low density tend to be in *enhancement mode*.<sup>24</sup> Firstly, the drain-source current of a sensor was monitored in various concentrations of Hg<sup>2+</sup> ions in water-droplets to characterize the sensing process. Fig. 4c and the inset show the measured drain-source current and resistance of a sensor in different concentrations of Hg<sup>2+</sup> ions in water droplets. Initially, a small current ( $< 10^{-8}$  A) was only observed as we chose a SWNT FET in *enhancement mode*. When the concentration of solution reached about  $\sim 10$  nM, which is the allowable limit of Hg<sup>2+</sup> ions in drinking water set by most government environmental protection agencies, a noticeable change in the resistance was observed (see the inset in Fig. 4c). Sequential injections of Hg<sup>2+</sup> led to discreet changes of the resistance of the sensor. The working principle of our sensor is the difference in standard potential between SWNTs ( $E^0_{\text{SWNT}} = 0.5-0.8$  V *versus* NHE) and Hg<sup>2+</sup> ions ( $E^0_{\text{Hg}^{2+}} = 0.8535$  V *versus* NHE).<sup>25-27</sup>

By integrating NGs with a Hg<sup>2+</sup> sensor, we could build a self-powered environmental sensing device. Fig. 4d shows a circuit diagram. A light emitting diode was attached on the circuit to serve as an indicator for Hg<sup>2+</sup> detection. To accomplish self-powered sensing of environmental pollutants with NGs, a circuit was designed with two independent loops. In the energy harvesting process, a circuit was connected in loop 'A' (Fig. 4d) with NGs and rectifying diode bridge to store generated charge in the capacitor (1000 µF, Nichicon). After a sufficient charging process, the connection was changed to loop 'B' in Fig. 4d, thus it was ready to detect Hg<sup>2+</sup> ions and light up an LED with a certain intensity depending on the concentration of pollutants in the water droplet. As a proof of concept, we demonstrated an

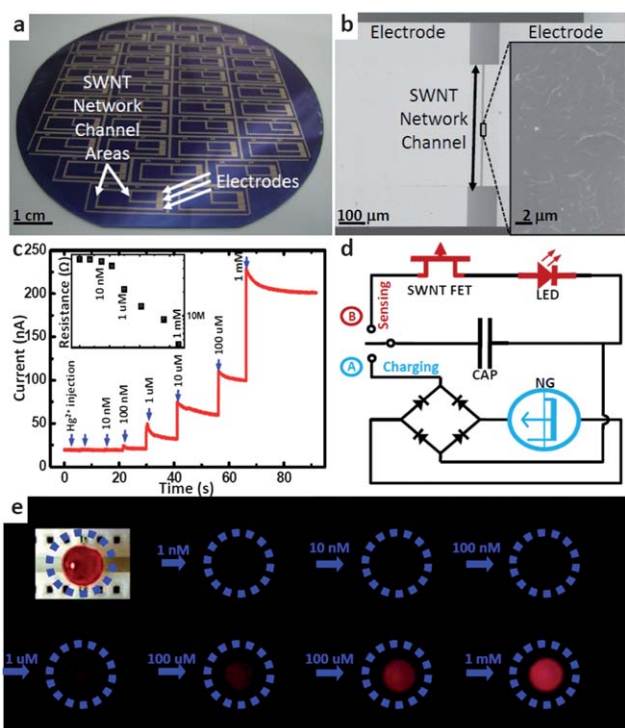


**Fig. 4** Characteristics of a self-powered  $\text{Hg}^{2+}$  sensor driven by nanogenerators. (a) Optical image of fabricated sensor array on a 4 inch silicon wafer. (b) SEM image of single-walled carbon nanotube network in a sensor. (c) Sensing behaviour of our fabricated sensor with various concentrations of  $\text{Hg}^{2+}$  ions in water solution. The inset shows the plot of resistance depending on mercury ion injection. (d) Circuit diagram depicting our self-powered sensor composed of a nanogenerator, a rectifying bridge, a capacitor, a  $\text{Hg}^{2+}$  detector and a light emitting diode with the (A) charging and (B) sensing process selecting switch. (e) Optical images of a laser emitting diode representing intensity changes owing to resistance changes in the detector depending on the concentration of  $\text{Hg}^{2+}$  ions in water solution. All measurements were conducted with energy stored by nanogenerators.

environmental sensor circuit fully powered by NGs which also can give us the result of detection simultaneously without any supporting equipment. Fig. 4e shows photograph images of an LED that was lit up under each concentration of  $\text{Hg}^{2+}$  ions in the water droplets. In this experiment, six capacitors were charged individually for  $\sim 1$  h using 10-layer integrated NGs (10 Hz, 1.2 cm peak-to-peak vibration distance, Labworks Inc.). Charged capacitors were connected in series to supply sufficient voltage ( $\sim 3$  V) for operation of a SWNT FET-based sensor and an LED all together. There was no external electric power source in our system.  $\text{Hg}^{2+}$  ions were injected in water droplets in sequential steps from 1 nM to 1 mM. All detection procedures were conducted for  $\sim 30$  s to observe intensity changes of the LED under constant power from capacitors. To minimize any power dissipation during sequential detection procedures, observation started from low concentration to high concentration. At lower concentrations of  $\text{Hg}^{2+}$  ions in water droplets, less power ( $V^2/R$ ) was expected to be used for the sensing operation due to the relatively high resistance in the circuit (see also Fig. 4c (inset) and d). As shown after the third image of Fig. 4e, noticeable LED light appeared from the concentration of 10 nM and got brighter gradually until those of

1 mM. Note that this detection experiment was conducted only utilizing our sensing circuit powered by NGs without any auxiliary equipment such as voltage or current signal amplifiers. In addition, the LED can be replaced by an RF unit so that the signal can be detected wirelessly over a longer distance. In the future, our system can be a prototype for environmental sensors which are stand-alone, self-powering and self-indicating.

## Conclusions

In summary, we have successfully fabricated a stand-alone, NG-powered mercury sensor utilizing ZnO NW-based generators and a SWNT-based  $\text{Hg}^{2+}$  ion detector. Here, harvested energy from high-performance NGs was able to power all detection operation and light up an LED indicator consequently. NGs were composed of 10-layers of a ZnO NW array and Au film both on flexible substrates which increased the number of effective contacts. We could utilize a SWNT FET as a  $\text{Hg}^{2+}$  sensor owing to the difference in standard potential between SWNTs and  $\text{Hg}^{2+}$  ions. The SWNT sensor served as a switch in our designed circuit, so that it turned on an attached LED when  $\text{Hg}^{2+}$  ions were detected in water solution. Significantly, without any support equipment, detection and LED lighting-up were successfully powered only by energy harvested via NGs. It implies that high performance NGs are not only able to power a detecting nano-device but also powerful enough to show the result of detection in a microscopic way. This work will inspire the development of a future self-powered sensor for unreachable and access-denied extreme environments.

## Notes and references

- Z. L. Wang and J. Song, *Science*, 2006, **312**, 242.
- F. A. Ponce and D. P. Bour, *Nature*, 1997, **386**, 351.
- C.-T. Huang, J. Song, W.-F. Lee, Y. Ding, Z. Gao, Y. Hao, L.-J. Chen and Z. L. Wang, *J. Am. Chem. Soc.*, 2010, **132**, 4766.
- C. Chang, V. H. Tran, J. Wang, Y.-K. Fuh and L. Lin, *Nano Lett.*, 2010, **10**, 726.
- S. Xu, Y. Qin, C. Xu, Y. Wei, R. Yang and Z. L. Wang, *Nat. Nanotechnol.*, 2010, **5**, 366.
- G. Zhu, R. Yang, S. Wang and Z. L. Wang, *Nano Lett.*, 2010, **10**, 3151.
- Y. Hu, Y. Zhang, C. Xu, G. Zhu and Z. L. Wang, *Nano Lett.*, 2010, **10**, 5025.
- Y. F. Lin, J. H. Song, Y. Ding, S. Y. Lu and Z. L. Wang, *Appl. Phys. Lett.*, 2008, **92**, 022105.
- Z. L. Wang, *Sci. Am.*, 2008, **298**, 82.
- X. Wang, J. Song, J. Liu and Z. L. Wang, *Science*, 2007, **316**, 102.
- Z. L. Wang, *Nano Today*, 2010, **5**, 540.
- K. Kasemets, A. Ivask, H.-C. Dubourguier and A. Kahru, *Toxicol. in Vitro*, 2009, **23**, 1116.
- J. Zhou, N. Xu and Z. L. Wang, *Adv. Mater.*, 2006, **18**, 2432.
- Z. Li, R. Yang, M. Yu, F. Bai, C. Li and Z. L. Wang, *J. Phys. Chem. C*, 2009, **112**, 20114.
- Y. Qi and M. C. McAlpine, *Energy Environ. Sci.*, 2010, **3**, 1275.
- A. Bachtold, P. Hadley, T. Nakanishi and C. Dekker, *Science*, 2001, **294**, 1317.
- T. H. Kim, J. Lee and S. Hong, *J. Phys. Chem. C*, 2009, **113**, 19393.
- M. Lee, J. Lee, T. H. Kim, H. Lee, B. Y. Lee, J. Park, Y. M. Jhon, M.-J. Seong and S. Hong, *Nanotechnology*, 2010, **21**, 055504.
- L. Vayssieres, *Adv. Mater.*, 2003, **15**, 464.
- J.-Y. Kim, C. S. Lee, J. H. Han, J. W. Cho and J. Bae, *Electrochem. Solid-State Lett.*, 2011, **14**, 56.
- J. Bae, M. K. Song, Y. J. Park, J. M. Kim, M. Liu and Z. L. Wang, *Angew. Chem., Int. Ed.*, 2011, **50**, 1.
- S. Rao, L. Huang, W. Setyawan and S. Hong, *Nature*, 2003, **425**, 36.
- M. Lee, J. Im, B. Y. Lee, S. Myung, J. Kang, L. Huang, Y.-K. Kwon and S. Hong, *Nat. Nanotechnol.*, 2006, **1**, 66.

- 
- 24 C. Kocabas, N. Pimparkar, O. Yesilyurt, S. J. Kang, M. A. Alam and J. A. Rogers, *Nano Lett.*, 2007, **7**, 1195.
- 25 P. W. Barone, S. Baik, D. A. Heller and M. S. Strano, *Nat. Mater.*, 2005, **4**, 86.
- 26 H. C. Choi, M. Shim, S. Bangsaruntip and H. J. Dai, *J. Am. Chem. Soc.*, 2002, **124**, 9058.
- 27 P. Patnaik and J. A. Dean, *Dean's Analytical Chemistry Handbook*, McGraw-Hill, New York, 2nd edn, 2004, section 13.